Supplementary Material

1 POPULATION DYNAMICS

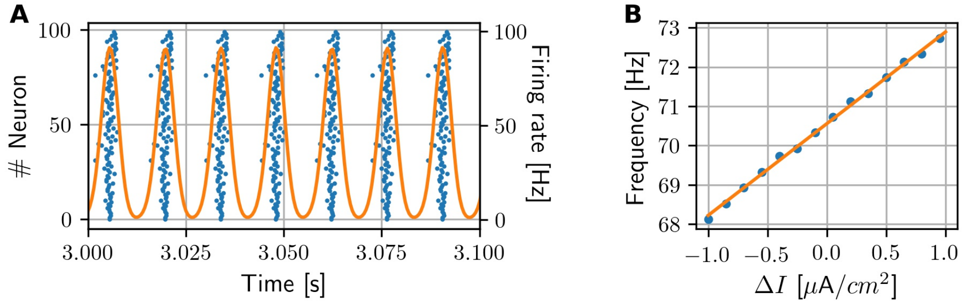

Figure S1. Raster plot and firing rate of one isolated neural population with $I = I_0$ = 11 μA/cm^2 (A). Linear dependency of the oscillating population frequency on the detuning $\Delta I = I - I_0$ (B).

2 V-MOTIF: SYNCHRONIZATION AND PHASE-LOCKING

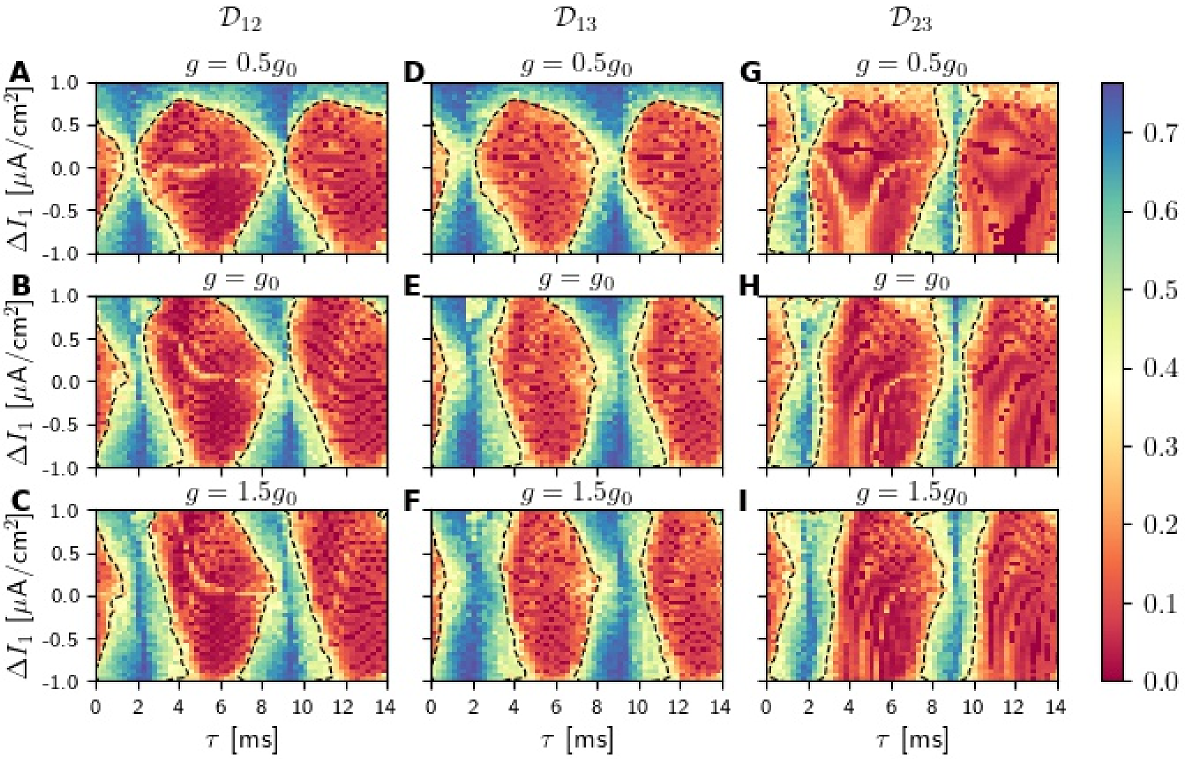

Figure S2. V-motif: Phase locking between population 1 and 2 (A-C), population 1 and 3 (D-F), and population 2 and 3 (G-I) as a function of the delay τ and the frequency mismatch ΔI in population 1 for different values of the synaptic strength g. The phase locking is measured with the index $\mathcal{D}_{ij}$ which implies a better locking as its value is closer to zero (see Methods in the main text).

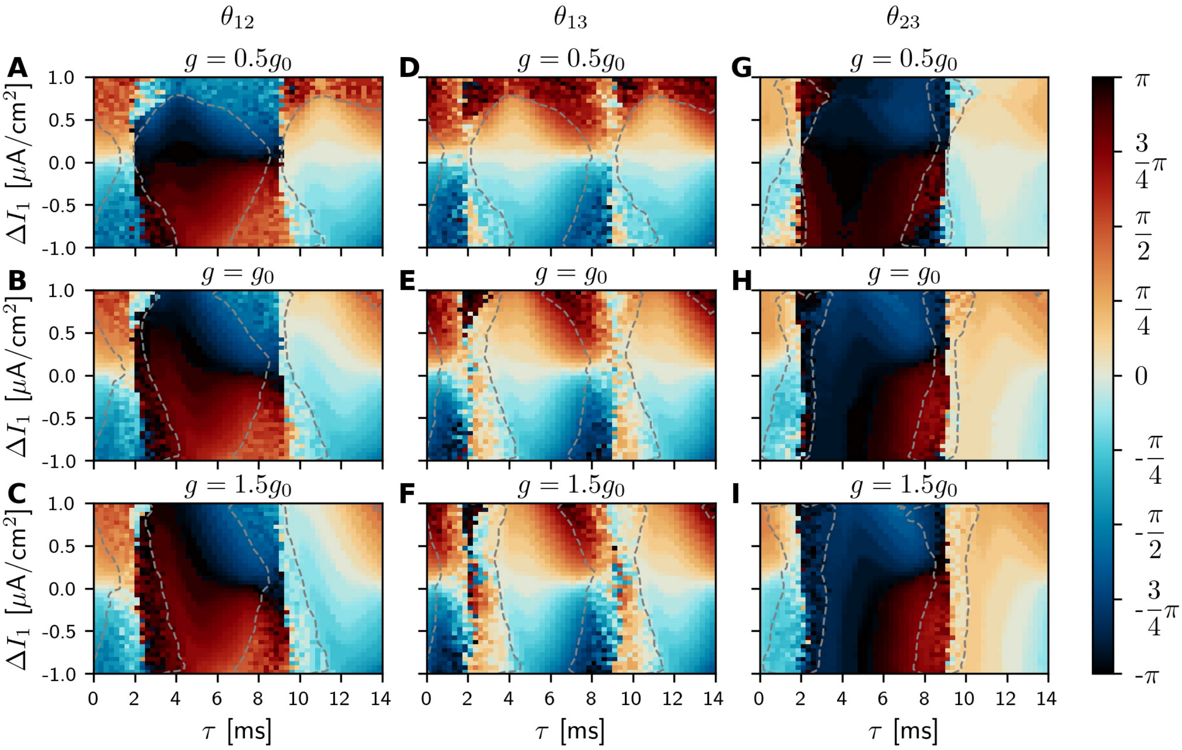

Figure S3. V-motif: Phase difference between population 1 and 2 θ_{12} (A-C), population 1 and 3 θ_{13} (D-F), and population 2 and 3 θ_{23} (G-I) as a function of the delay τ and the frequency mismatch ΔI in population 1 for different values of the synaptic strength g.

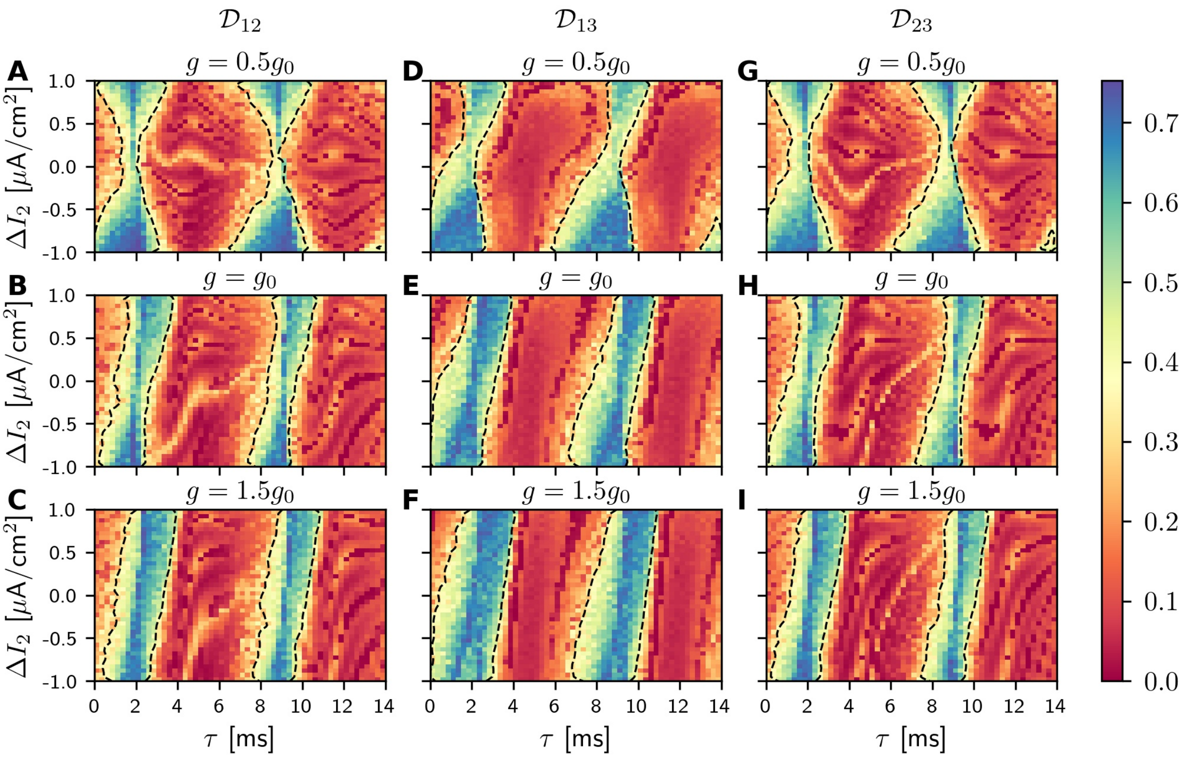

Figure S4. V-motif: Phase locking between population 1 and 2 (A-C), population 1 and 3 (D-F), and population 2 and 3 (G-I) as a function of the delay τ and the frequency mismatch ΔI in population 2 for different values of the synaptic strength g.

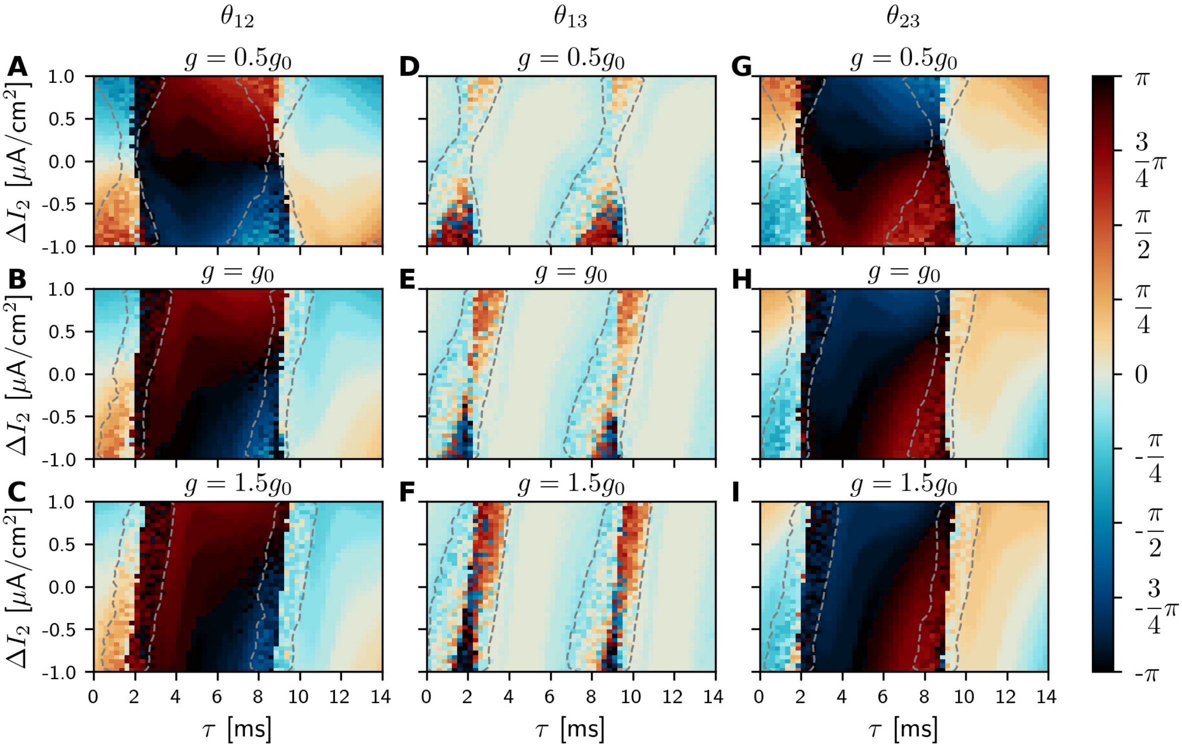

Figure S5. V-motif: Phase difference between population 1 and 2 θ_{12} (A-C), population 1 and 3 θ_{13} (D-F), and population 2 and 3 θ_{23} (G-I) as a function of the delay τ and the frequency mismatch ΔI in population 2 for different values of the synaptic strength g.

3 V-MOTIF: INFORMATION TRANSMISSION

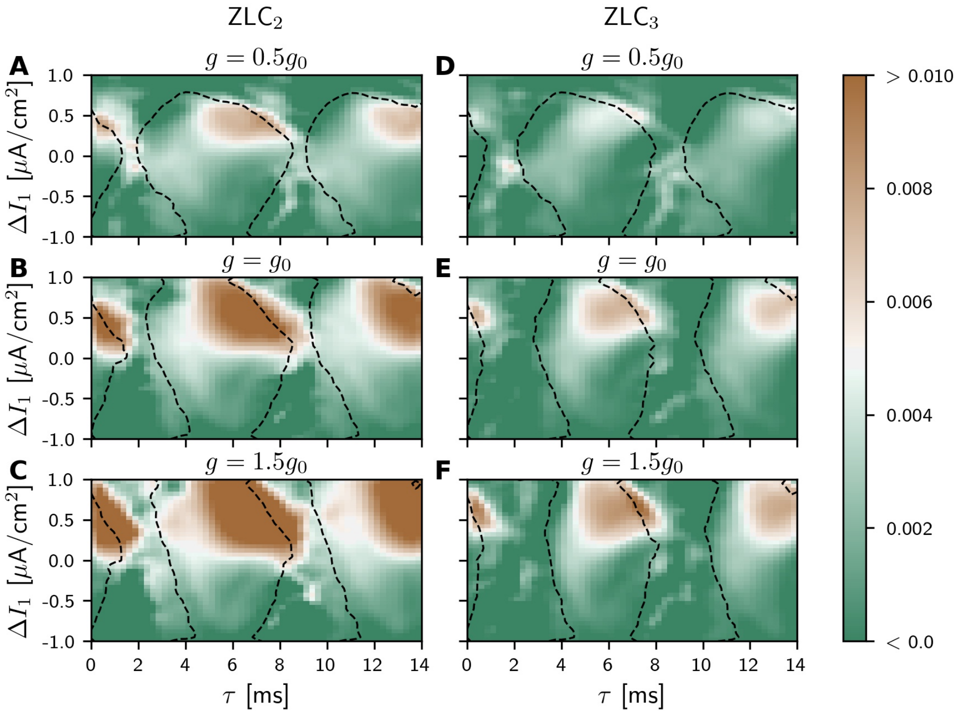

Figure S6. V-motif: Zero-lag cross covariance (ZLC) of the firing rates of the second (A-C) and third (D-F) population with the slow modulation injected as function of the delay τ and the frequency mismatch ΔI in population 1 for different values of the synaptic strength g.

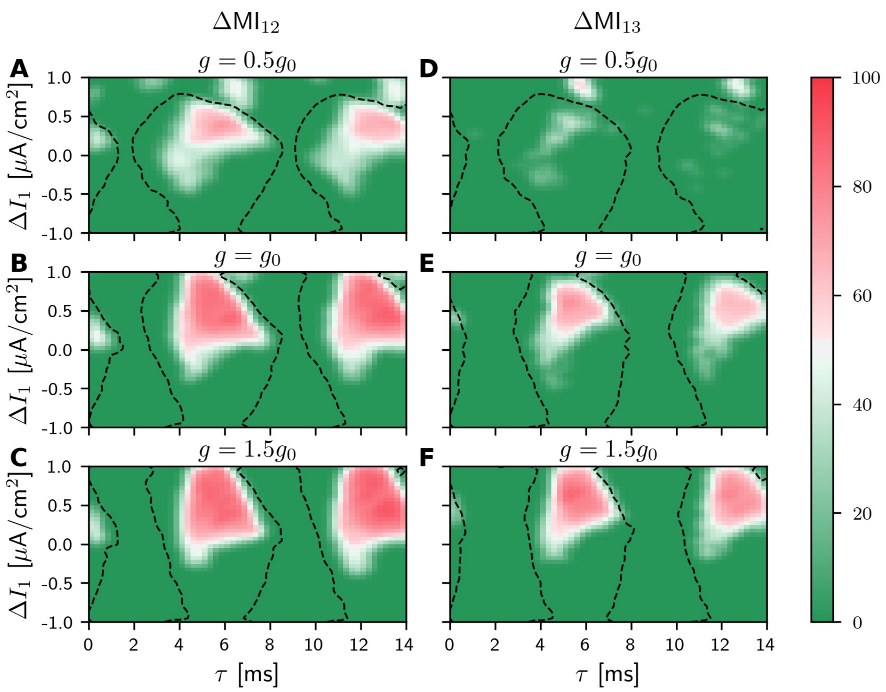

Figure S7. V-motif: Difference $\Delta\mathrm{MI}_{ij}$ between the firing rates of population 1 and 2 (A-C) and population 1 and 3 (D-F) when a slow modulation is injected as a function of the delay τ and the frequency mismatch ΔI in population 1 for different values of the synaptic strength g.

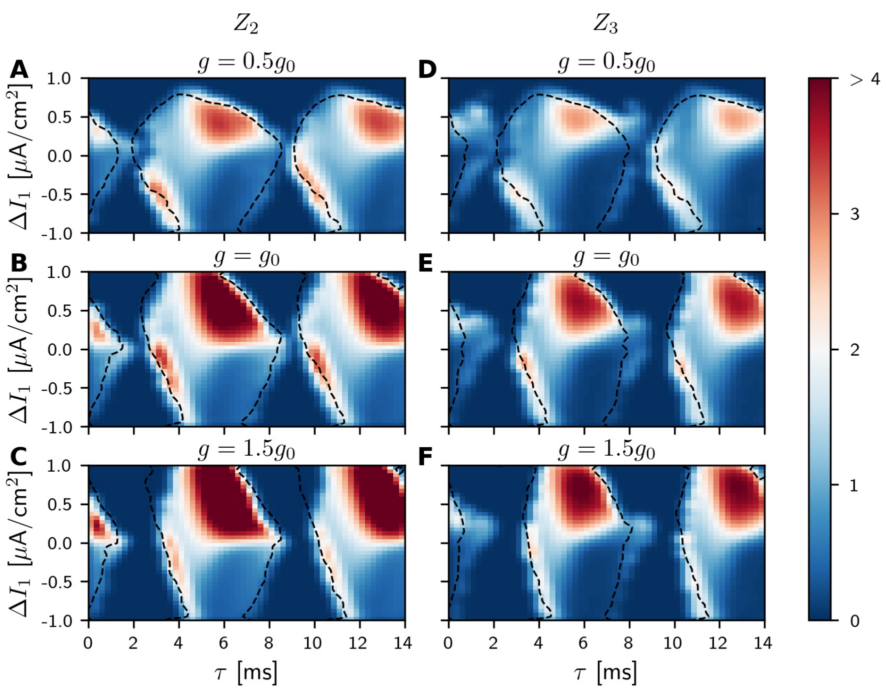

Figure S8. V-motif: Integral of the absolute value of the nPRC of the population 2 (A-C) and population 3 (D-F) when a fast signal is injectd as a function of the delay τ and the frequency mismatch ΔI in population 1 for different values of the synaptic strength g.

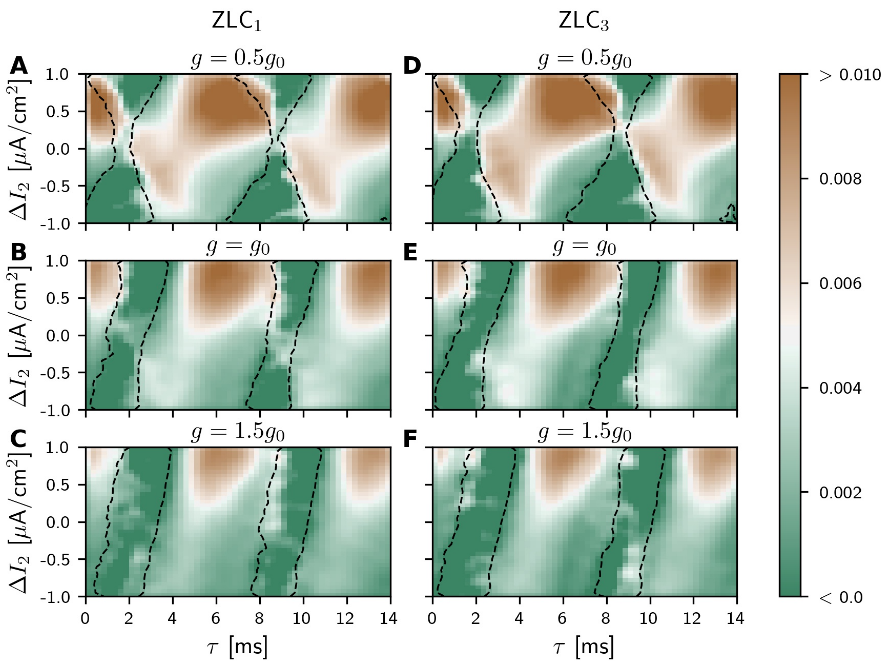

Figure S9. V-motif: Zero-lag cross covariance (ZLC) of the firing rates of the first (A-C) and third (D-F) population with the slow modulation injected as function of the delay τ and the frequency mismatch ΔI in population 2 for different values of the synaptic strength g.

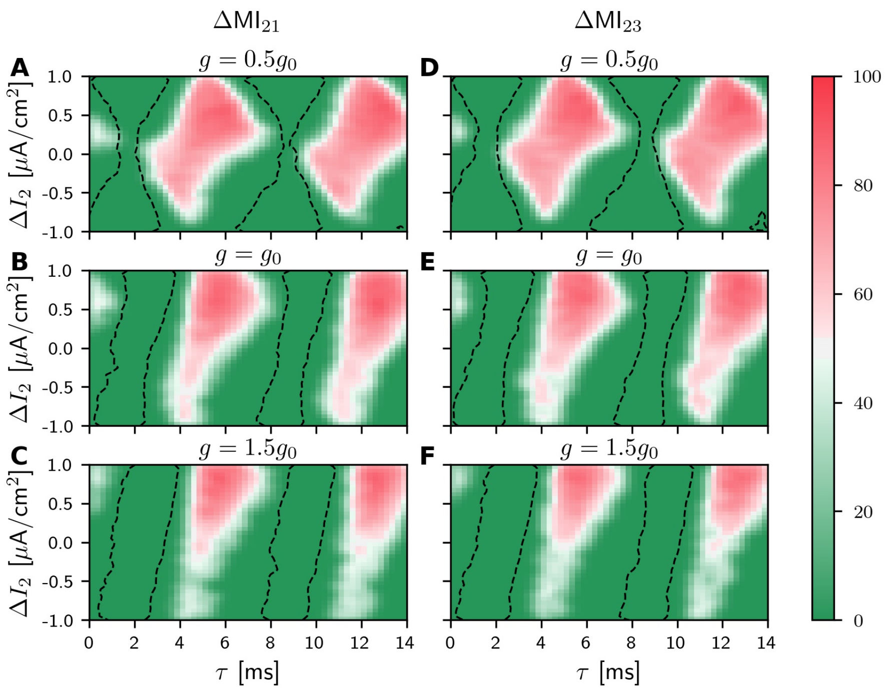

Figure S10. V-motif: Difference $\Delta \mathrm{MI}_{ij}$ between the firing rates of population 2 and 1 (A-C) and population 2 and 3 (D-F) when a slow modulation is injected as a function of the delay τ and the frequency mismatch ΔI in population 2 for different values of the synaptic strength g.

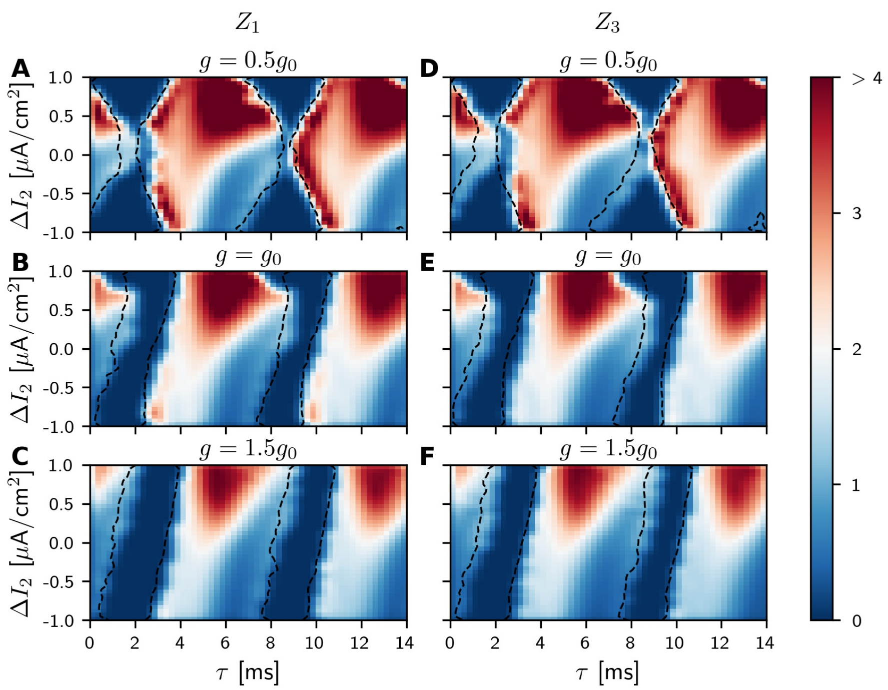

Figure S11. V-motif: Integral of the absolute value fo the nPRC of the population 1 (A-C) and population 3 (D-F) when a fast modulation is injected as a function of the delay τ and the frequency mismatch ΔI in population 2 for different values of the synaptic strength g.

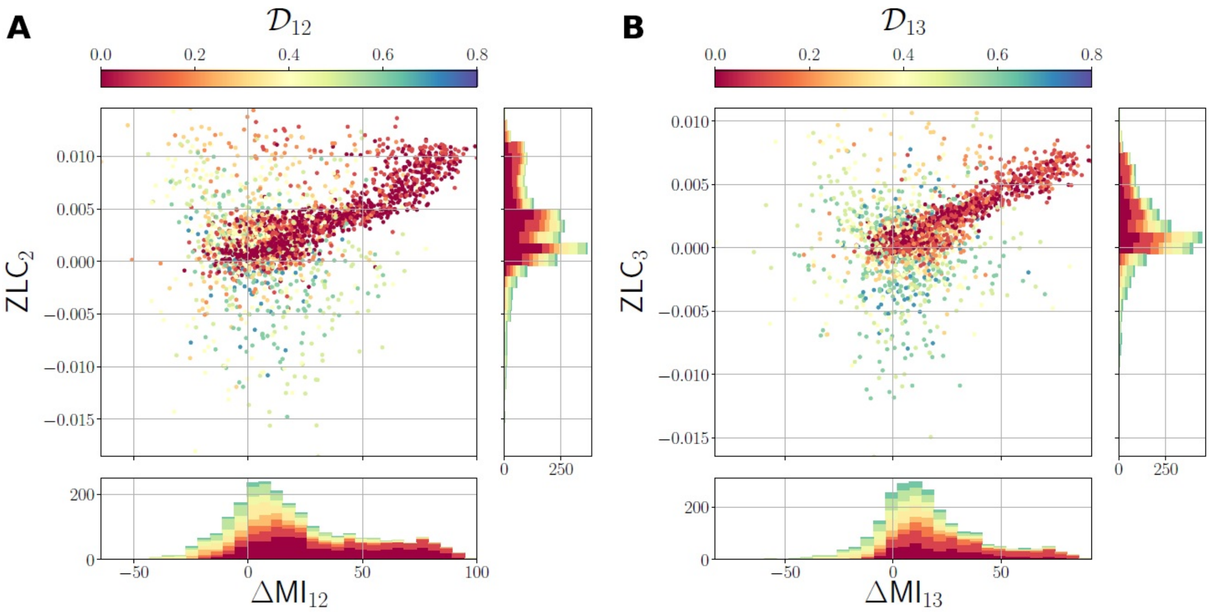

Figure S12. V-motif: Histograms of ZLC_i and $\Delta\mathrm{MI}_{1i}$ (i=2,3) as a function of the phase-locking index $\mathcal{D}$, for $g = g_0$. From the central plot, one can see how both measurements are non-linearly correlated when the phase-locking index is proximal to zero (perfect locking). Furthermore, high values of both measurements coincide with almost zero values of $\mathcal{D}$, implying that a better communication is achieved when the sender and receptor exhibit a constant phase difference relation.

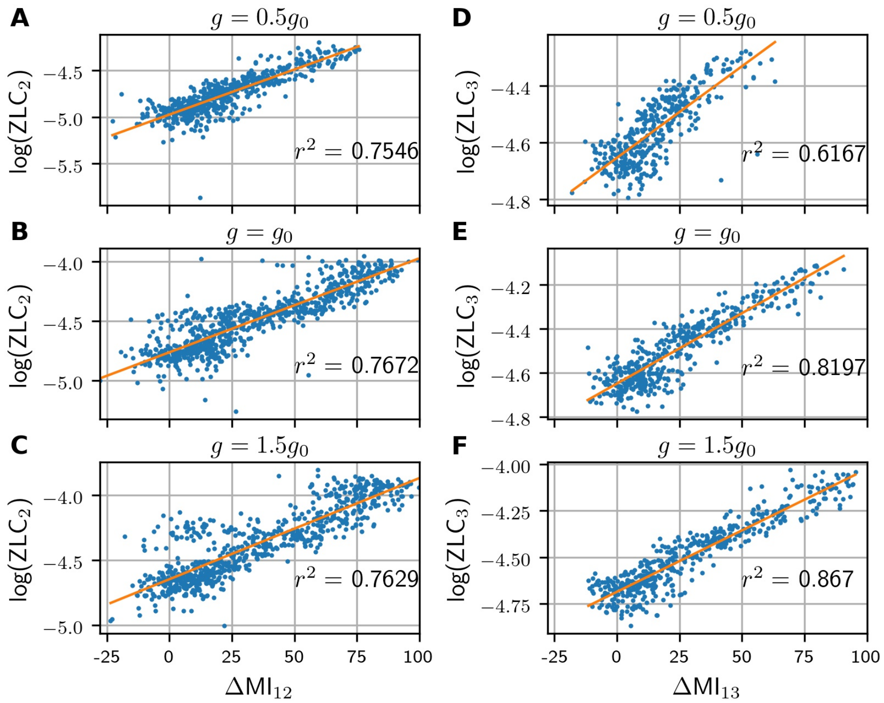

Figure S13. V-motif: R-squared regression of the natural logarithmic of ZLC_i and $\Delta\mathrm{MI}_{1i}$ (i = 2,3) for values of the phase-locking index $\mathcal{D}$ lower than 0.25. To avoid indeterminations, a bias term has been added to ZLC_i values before computing the logarithmic. This confirms the relation observerd in S12 between these two measurement over the condition of $\mathcal{D}$ being proximal to zero.

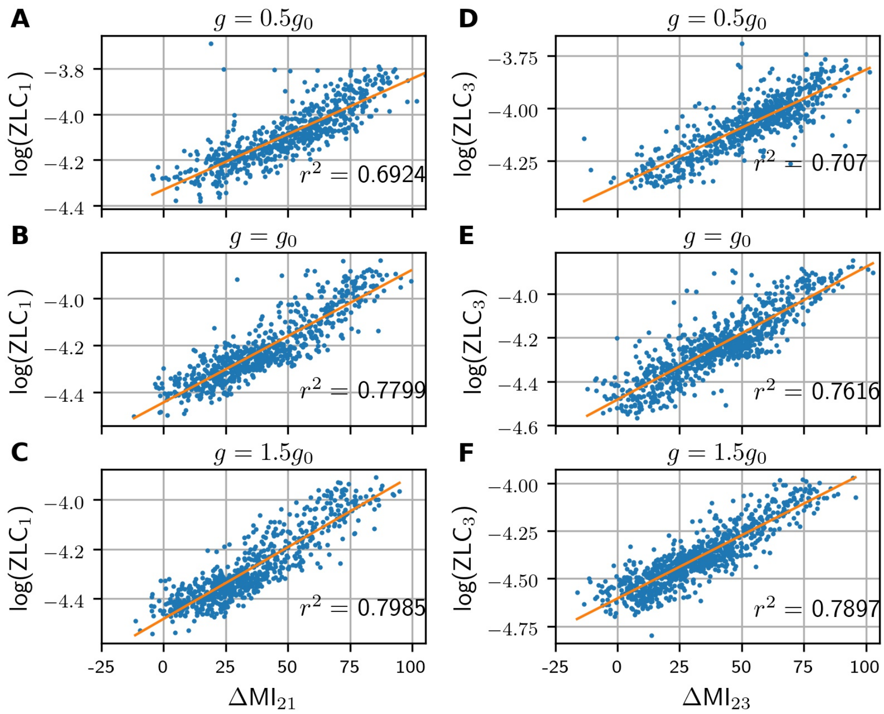

Figure S14. V-motif: R-squared regression of the natural logarithmic of ZLC_i and $\Delta\mathrm{MI}_{2i}$ (i = 1,3) for values of the phase-locking index $\mathcal{D}$ lower than 0.25. To avoid indeterminations, a bias term has been added to ZLC_i values before computing the logarithmic.

4 CIRCULAR MOTIF: SYNCHRONIZATION AND PHASE-LOCKING

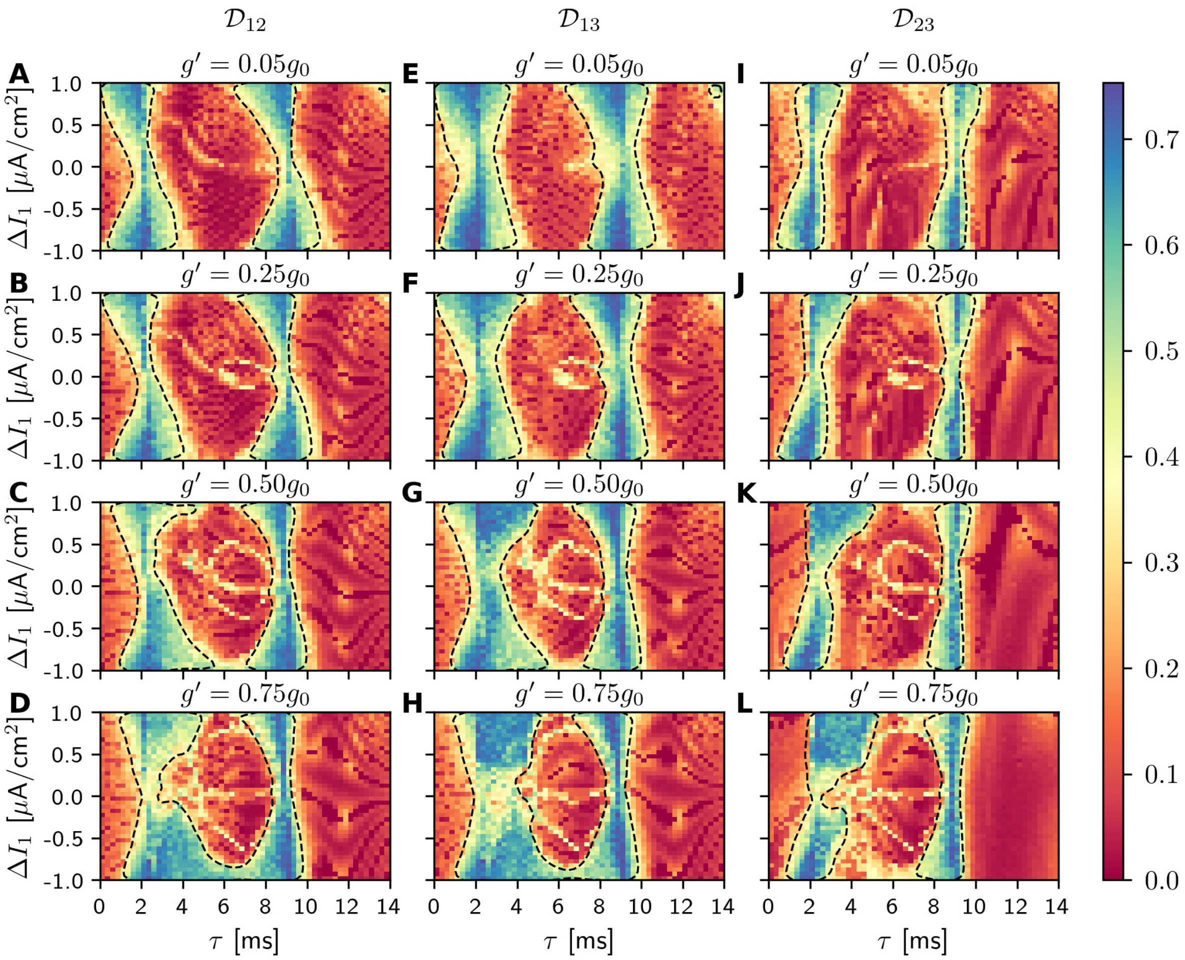

Figure S15. Circular motif: Phase locking between population 1 and 2 (A-D), population 1 and 3 (E-H), and population 2 and 3 (I-K) as a function of the delay τ and the frequency mismatch ΔI in population 1 for different values of the synaptic strength g'.

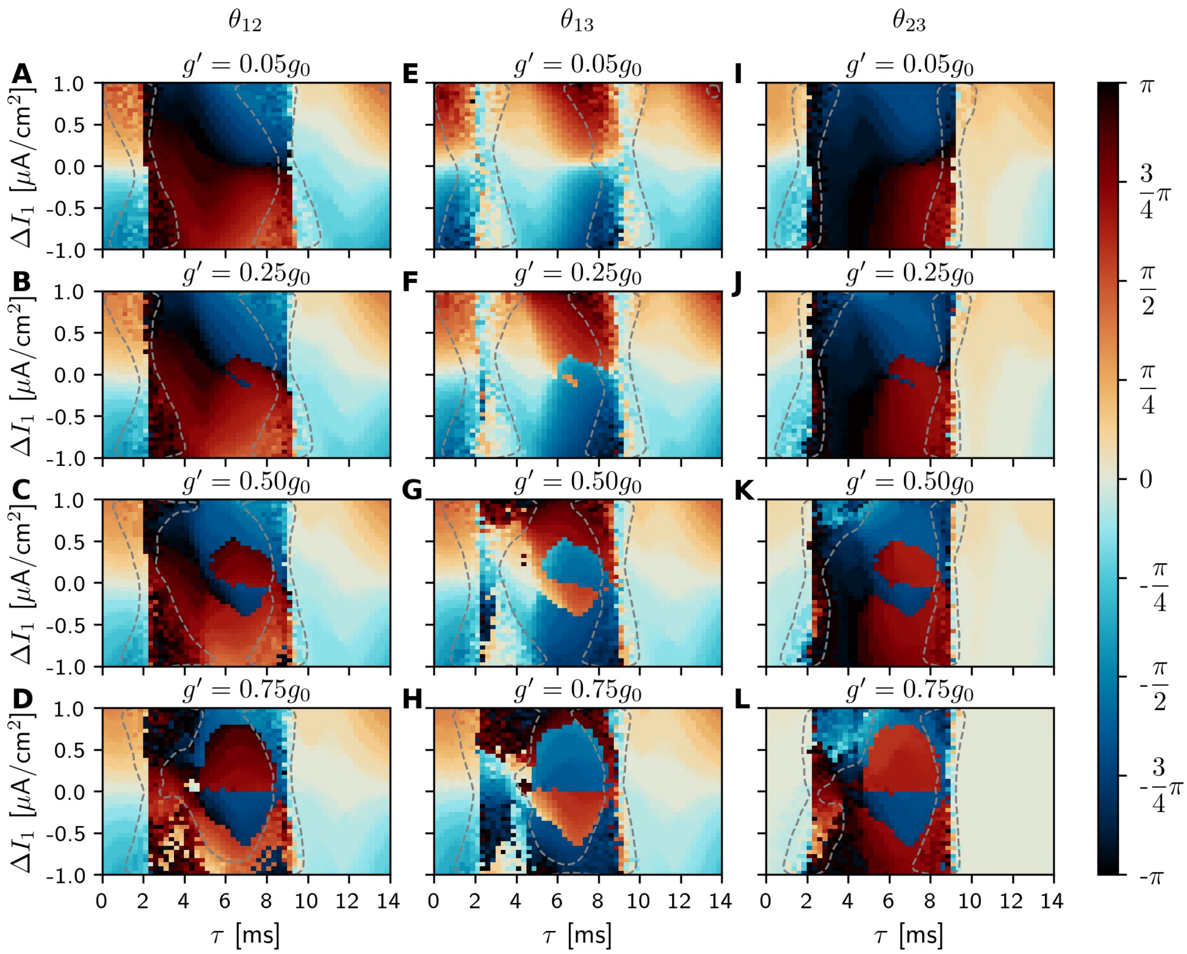

Figure S16. Circular motif: Phase difference between population 1 and 2 θ_{12} (A-D), population 1 and 3 θ_{13} (E-H), and population 2 and 3 θ_{23} (I-K) as a function of the delay τ and the frequency mismatch ΔI in population 1 for different values of the synaptic strength g'.

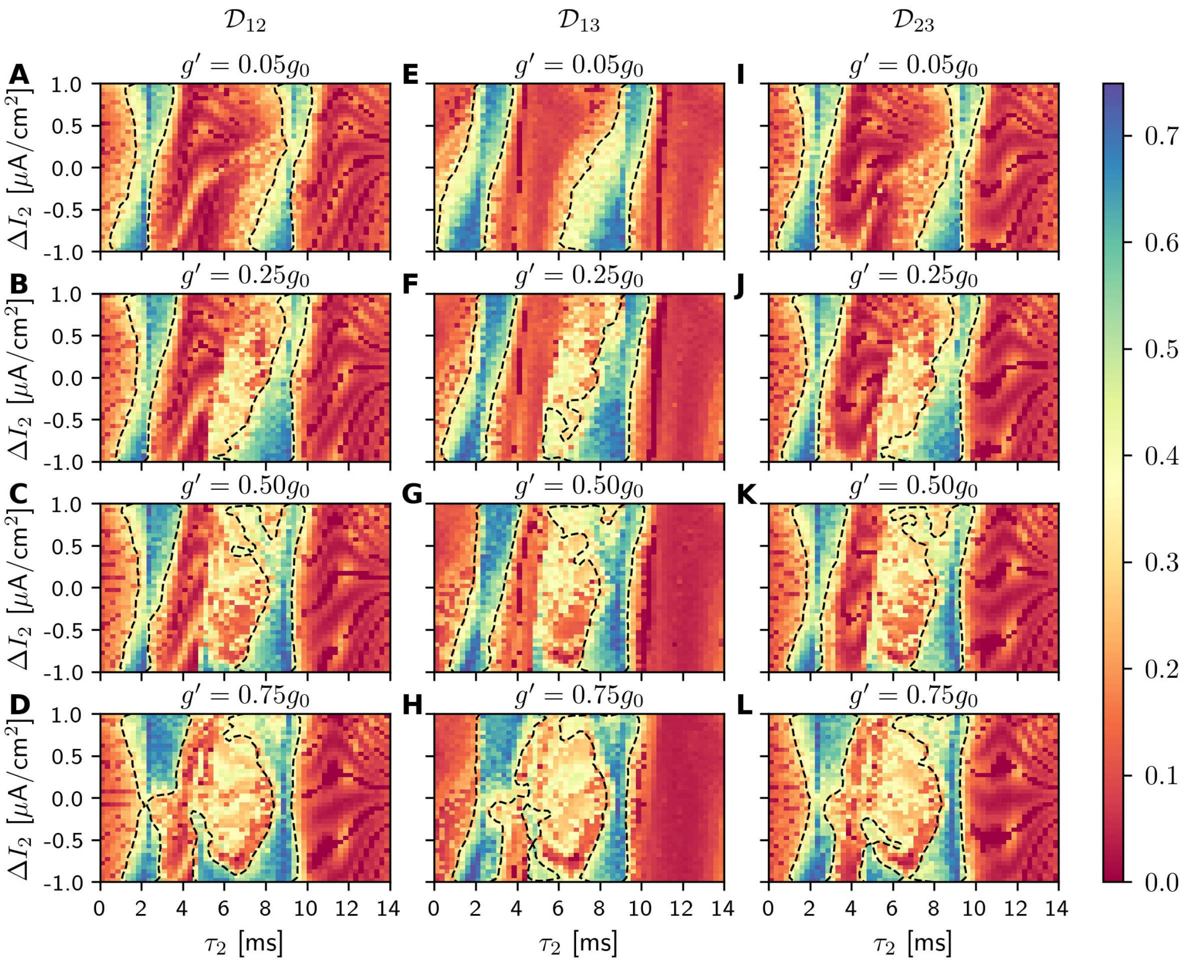

Figure S17. Circular motif: Phase locking between population 1 and 2 (A-D), population 1 and 3 (E-H), and population 2 and 3 (I-K) as a function of the delay τ and the frequency mismatch ΔI in population 2 for different values of the synaptic strength g.

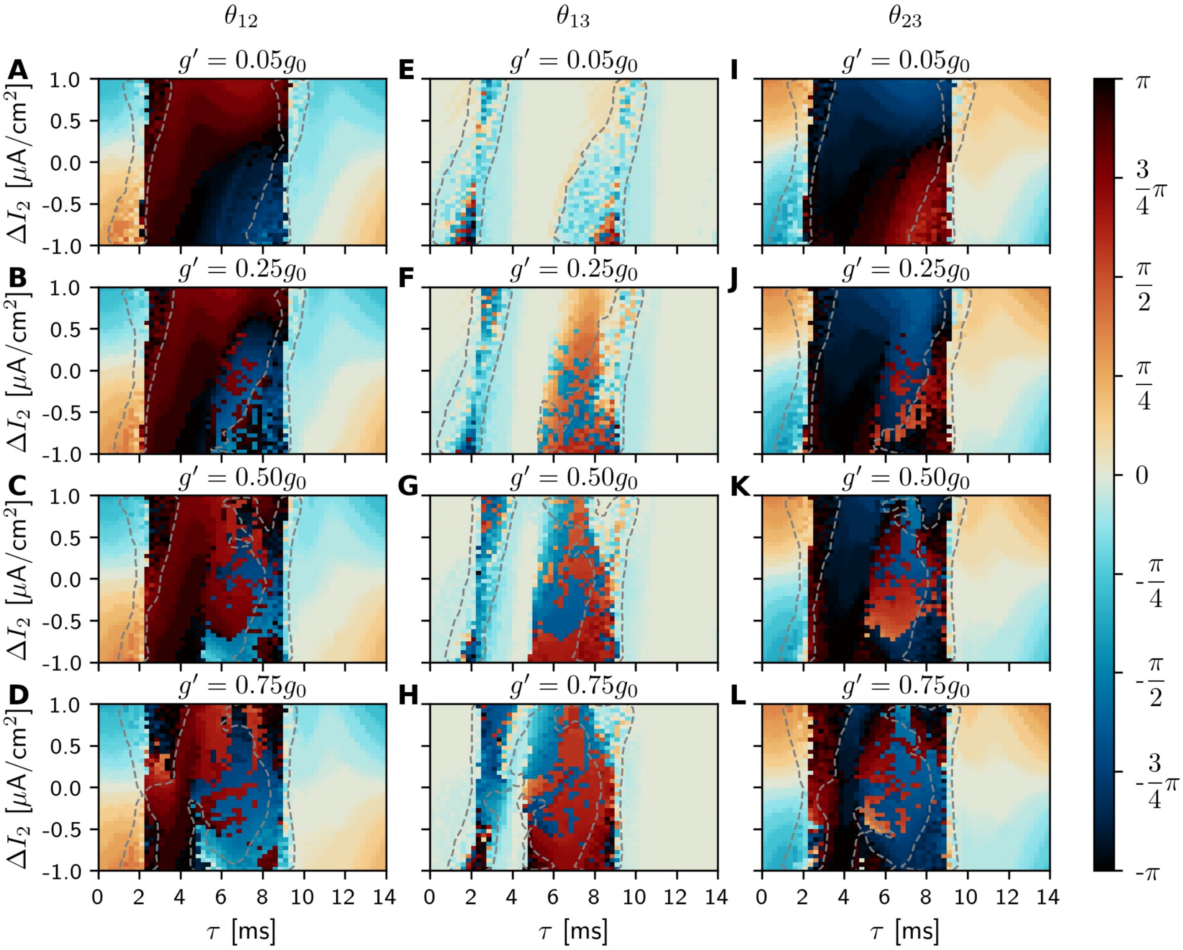

Figure S18. Circular motif: Phase difference between population 1 and 2 θ_{12} (A-D), population 1 and 3 θ_{13} (E-H),and population 2 and 3 θ_{23} (I-K) as a function of the delay τ and the frequency mismatch ΔI in population 2 for different values of the synaptic strength g'.

5 CIRCULAR MOTIF: INFORMATION TRANSMISSION

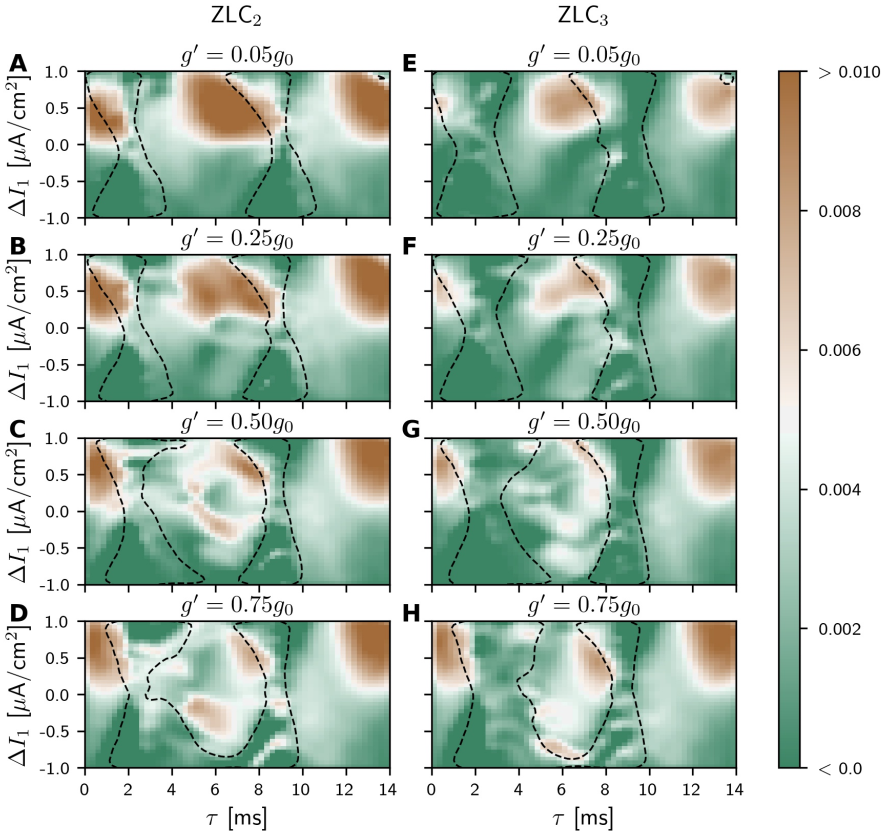

Figure S19. Circular motif: Zero-lag cross covariance (ZLC) of the firing rates of the first (A-D) and third (E-H) population with the slow modulation injected as function of the delay τ and the frequency mismatch ΔI in population 1 for different values of the synaptic strength g'.

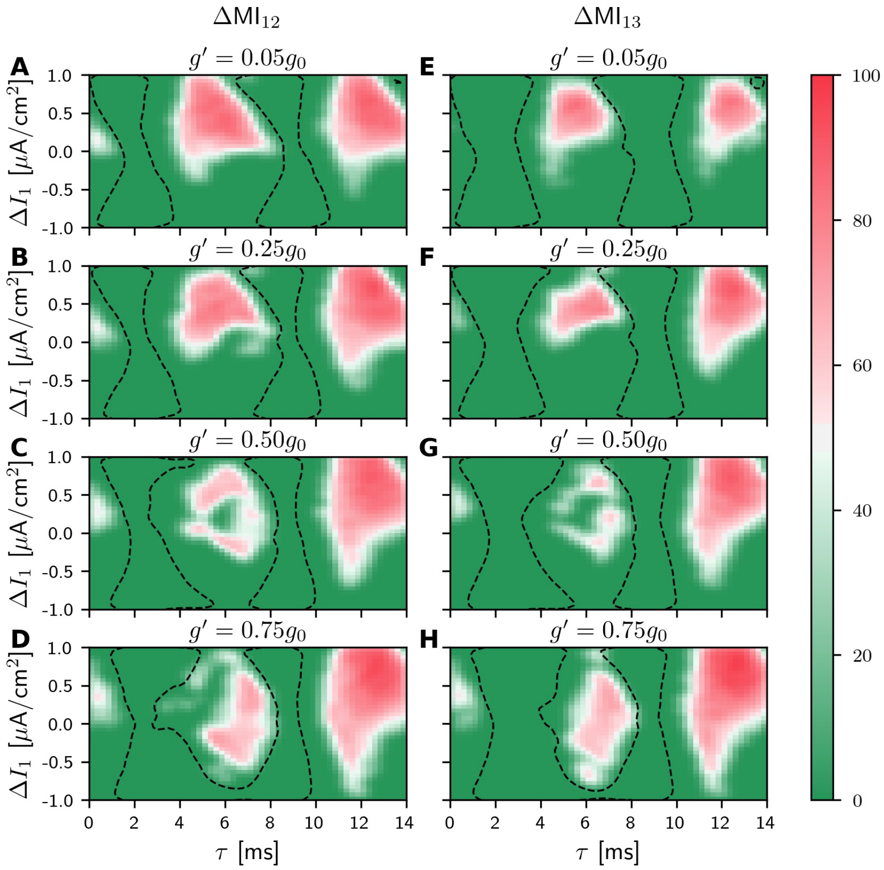

Figure S20. Circular motif: Difference $\Delta \mathrm{MI}_{ij}$ between the firing rates of population 1 and 2 (A-D) and population 1 and 3 (E-H) when a slow modulation is injected as a function of the delay τ and the frequency mismatch ΔI in population 1 for different values of the synaptic strength g.

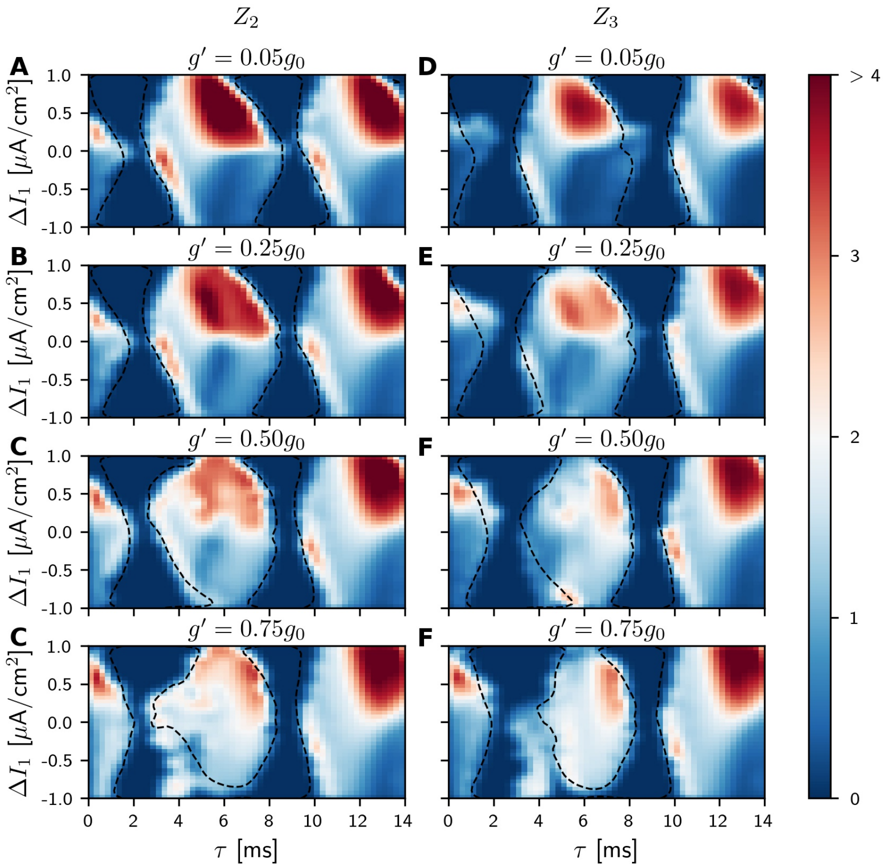

Figure S21. Circular motif: Integral of the absolute value of the nPRC of the population 2 (A-D) and population 3 (E-H) when a fast signal is injected as a function of the delay τ and the frequency mismatch ΔI in population 1 for different values of the synaptic strength g.

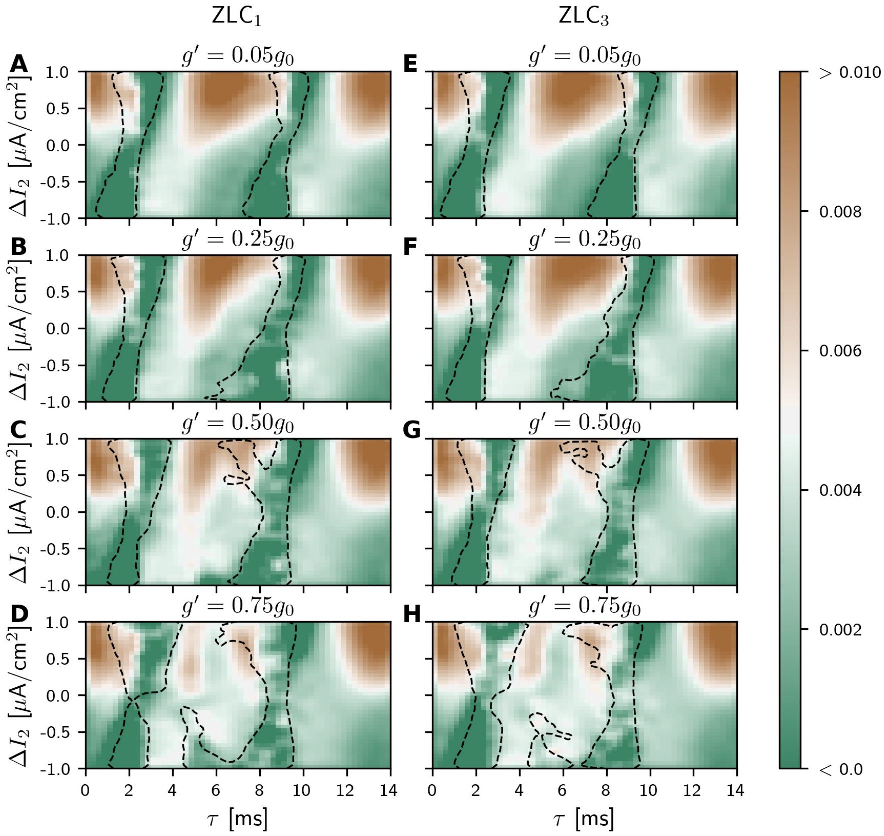

Figure S22. Circular motif: Zero-lag cross covariance (ZLC) of the firing rates of the first (A-D) and third (E-H) population with the slow modultion injected as function of the delay τ and the frequency mismatch ΔI in population 2 for different values of the synaptic strength g'.

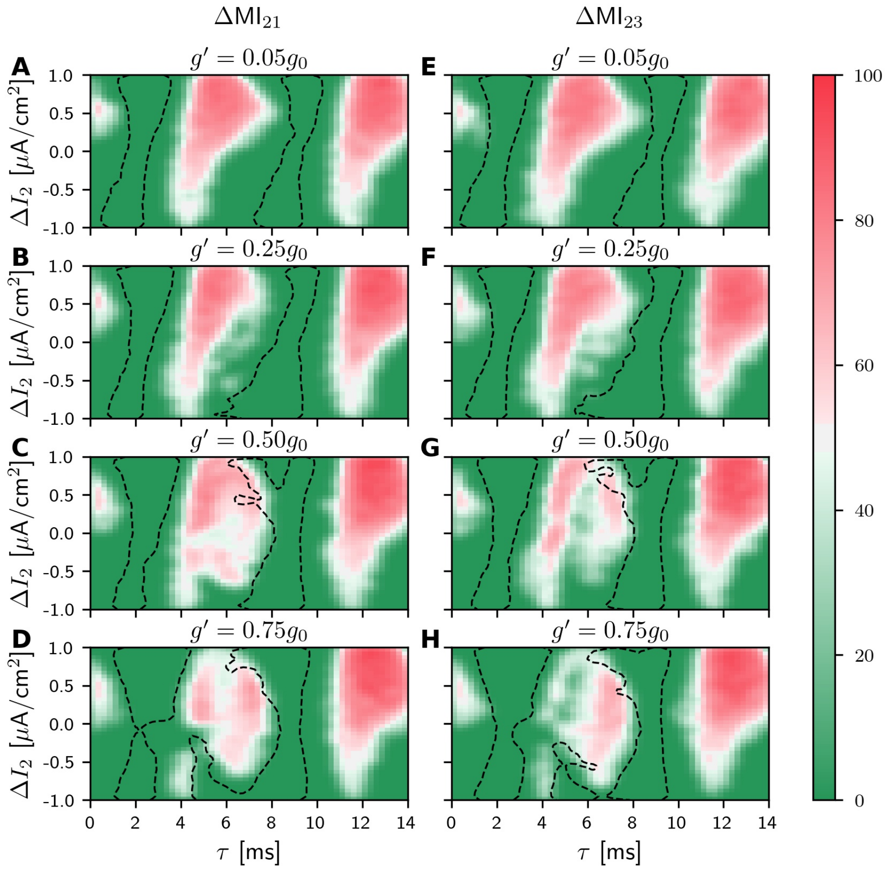

Figure S23. Circular motif: Difference $\Delta\mathrm{MI}_{ij}$ between the firing rates of population 2 and 1 (A-D) and population 2 and 3 (E-H) when a slow modulation is injected as a function of the delay τ and the frequency mismatch ΔI in population 2 for different values of the synaptic strength g.

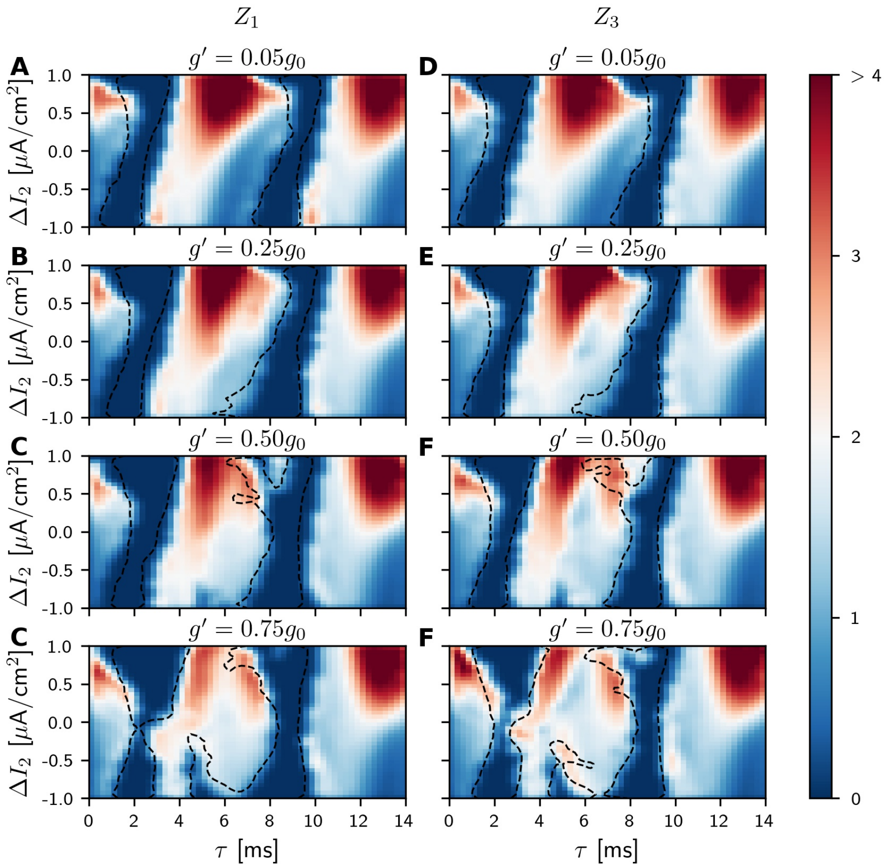

Figure S24. Circular motif: Integral of the absolute value fo the nPRC of the population 1 (A-D) and population 3 (E-H) when a fast signal is injected as a function of the delay τ and the frequency mismatch ΔI in population 2 for different values of the synaptic strength g.